Hindawi
Advances in Materials Science and Engineering
Volume 2018, Article ID 6158096, 5 pages
https://doi.org/10.1155/2018/6158096

Research Article

Novel Low-Permittivity $(Mg_{1-x}Cu_x)_2SiO_4$ Microwave Dielectric Ceramics

Chengxi Hu,[1] Yuan Liu,[2] Wujun Wang,[1] and Bo Yang[3]

[1] *Faculty of Science, Xi'an Aeronautical University, No. 259, West 2nd Ring, Xi'an 710077, China*
[2] *School of Physics and Information Technology, Shaanxi Normal University, Xi'an 710062, China*
[3] *Surface and Interface Science Laboratory, RIKEN, 2-1 Hirosawa, Wako-shi, Saitama 351-0198, Japan*

Correspondence should be addressed to Chengxi Hu; huchengxi@163.com

Received 22 November 2017; Revised 5 January 2018; Accepted 1 March 2018; Published 26 March 2018

Academic Editor: Francesco Ruffino

The effects of B_2O_3–LiF addition on the phase composition, microstructures, and microwave dielectric properties of $(Mg_{0.95}Cu_{0.05})_2SiO_4$ ceramics fabricated by a wet chemical method were studied in detail. The B_2O_3–LiF was selected as liquid-phase sintering aids to reduce the densification sintering temperature of $(Mg_{0.95}Cu_{0.05})_2SiO_4$ ceramics. The B_2O_3 6%–Li_2O 6%-modified $(Mg_{0.95}Cu_{0.05})_2SiO_4$ ceramics sintered at 1200°C possess good performance of $\varepsilon_r \sim 4.37$, $Q \times f \sim 36{,}700$ GHz and $\tau_f \sim 42$ ppm/°C.

1. Introduction

The rapid development in modern communications and Internet technology has created an urgent demand for the development of microwave ceramics [1–5]. Such microwave equipments require light weight, low loss, small size, and good temperature stability. Therefore, the materials used for the microwave substrates and dielectric resonators should have low dielectric constant (ε_r), high quality factor ($Q \times f$), and near-zero temperature coefficient of resonator frequency (τ_f). Mg_2SiO_4 is an essential material with low ε_r and high $Q \times f$. So it is considered to be a promising candidate as a low-dielectric-constant microwave material for applications in microwave substrates [2–9]. To our knowledge, the relation between the microwave dielectric properties and the structure for the Cu^{2+}-doped Mg_2SiO_4 system has not yet been investigated. Moreover, the sintering temperature of $(Mg_{1-x}Cu_x)_2SiO_4$ is too high in the recently reported microwave ceramics. Thus, 12 wt.% B_2O_3–LiF was used as sintering aids to reduce the densification sintering temperature down to a lower temperature range. In this work, we have reported the $(Mg_{1-x}Cu_x)_2SiO_4$ ceramics by a wet chemical process. The effects of additive B_2O_3–LiF on the phase compositions, microstructures, and microwave dielectric behavior were studied.

2. Experimental Procedure

SiO_2 nanospheres were prepared by the sol-gel method, and then the powders were used as raw material to synthesize the SiO_2-based ceramics. The microwave dielectric ceramics with high performance were successfully prepared in our previous work. The $(Mg_{1-x}Cu_x)_2SiO_4$ ceramics belong to SiO_2-based ceramics. Following the method of Hu et al. [1], it was quite expected to achieve success. All experiments were conducted in air. All reagents were analytical pure and used as received without further purification. $(Mg_{1-x}Cu_x)_2SiO_4$ powders were prepared using the sol-gel method. For this purpose, $Mg(NO_3)_2 \cdot 6H_2O$ and $CuSO_4 \cdot 5H_2O$ were dissolved individually in 100 ml ethanol and 10 ml distilled water and then added into the mixture under magnetic stirring, marked as A. Tetraethyl orthosilicate (TEOS) and $CuSO_4$ were used as received. The starting sol was prepared by hydrolysis of TEOS under magnetic stirring in the presence of 100 ml alcohol solution in 40°C water for 30 min, marked as B. Subsequently, the solution B was added to A by continuous vigorous magnetic stirring for 3 h at 40°C in water and then kept at 60°C overnight to allow gel formation. Finally, the obtained products were dried and calcined at 900°C for 4 h in an alumina crucible. The calcined powders were milled with ZrO_2 balls in ethanol for 12 h and dried to obtain

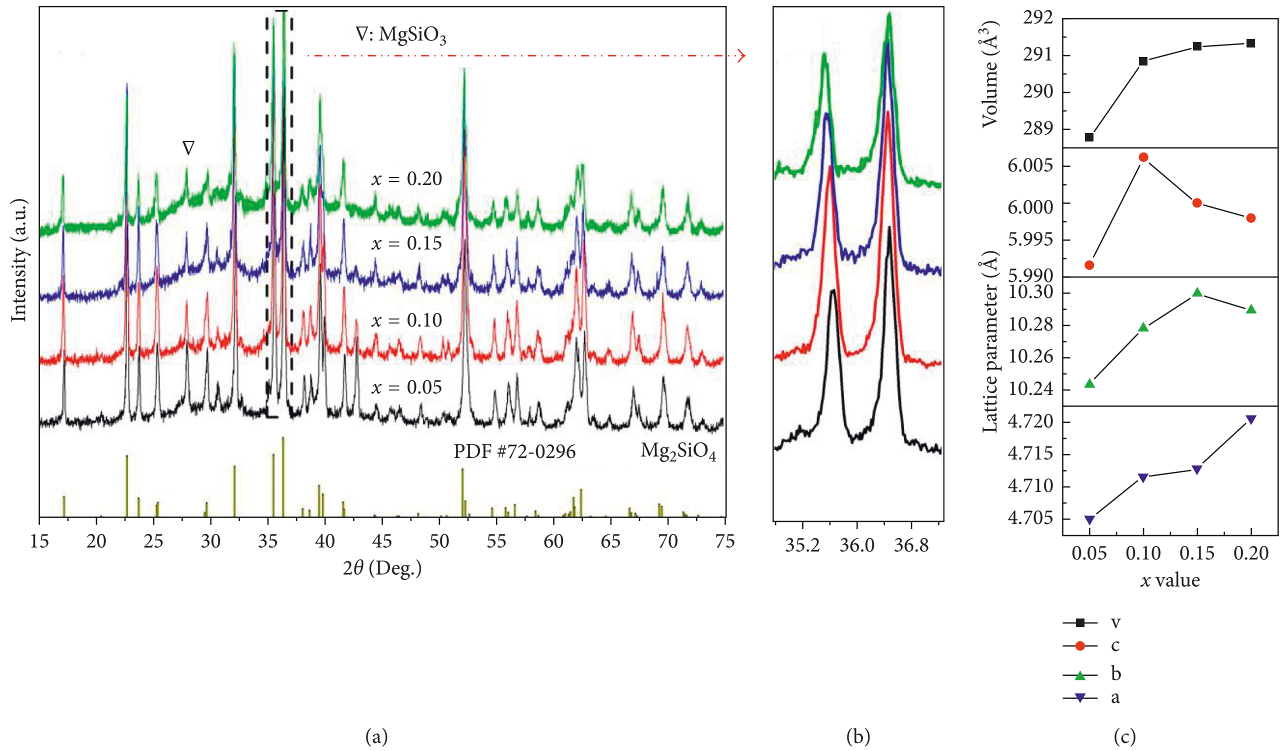

Figure 1: (a) XRD patterns of $(Mg_{1-x}Cu_x)_2SiO_4$ ($x = 0.05$–0.20) ceramics sintered at 1300°C for 4 h; (b) locally magnified peak profiles indicated in (a); (c) the lattice parameters as a function of the x value.

$(Mg_{1-x}Cu_x)_2SiO_4$ powders. The prepared powders were divided into two groups. The first group was not doped, while the second group was doped with B_2O_3–LiF. Both of them with polyvinyl alcohol water solution were pressed individually into cylindrical specimen with a diameter of 11.5 mm under a uniaxial pressure of 120 MPa. The undoped specimens were placed in an alumina crucible and heated to the sintering temperatures varying from room temperature to 1350°C with a rate of 5°C/min. After sintering for 4 h in air atmosphere, the specimens were freely cooled down to room temperature inside the furnace. The B_2O_3–LiF co-doped $(Mg_{1-x}Cu_x)_2SiO_4$ ceramics were sintered at 1000–1350°C for 4 h.

The crystalline-phase structure was identified by D/max-2550V/PC X-ray diffractometer (Rigaku, Tokyo, Japan) with Cu-$\kappa\alpha$ radiation (at 40 kv and 20 mA) at a scan rate $2\theta = 0.02\ s^{-1}$. The morphology of the samples was characterized by a scanning electron microscope (SEM, FEI-quanta 200, USA) and a high-resolution transmission electron microscope (JEM-2100, Japan). The X-ray photoelectron spectroscopy (XPS, Kratos Analytical Ltd., Japan) with a monochromatic Al was conducted to examine the microstructure for fracture surface of ceramics.

The bulk densities (ρ) of the samples were measured by the Archimedes method using distilled water as medium. The microstructures were observed on the as-sintered ceramic surfaces of samples by a scanning electron microscope (SEM, FEI-quanta 200, USA). The phase evolution of the $(Mg_{1-x}Cu_x)_2SiO_4$ ceramics was performed by XRD. The as-sintered cylindrical specimens with the thickness of about 5 mm and diameter of about 10 mm were used for evaluating the microwave dielectric

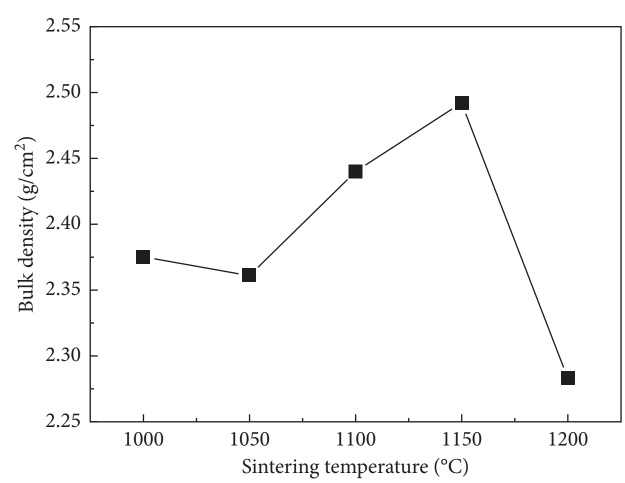

Figure 2: The variation of bulk density of $(Mg_{0.95}Cu_{0.05})_2SiO_4$ with 12% B_2O_3–LiF sintered at (a) 1000°C, (b) 1050°C, (c) 1100°C, (d) 1150°C, and (e) 1200°C.

properties. The dielectric constant and quality values were determined by the $TE_{01\delta}$ shielded cavity method using a vector network analyzer (ZVB20, Rohde & Schwarz, Munich, Germany). The temperature coefficient of the resonant frequency (τ_f) was calculated with the following formula:

$$\tau_f = \frac{f_{80} - f_{25}}{f_{25} \times (80 - 25)}, \quad (1)$$

where f_{25} and f_{80} represent the $TE_{01\delta}$ resonant frequency measured at 25°C and 80°C, respectively.

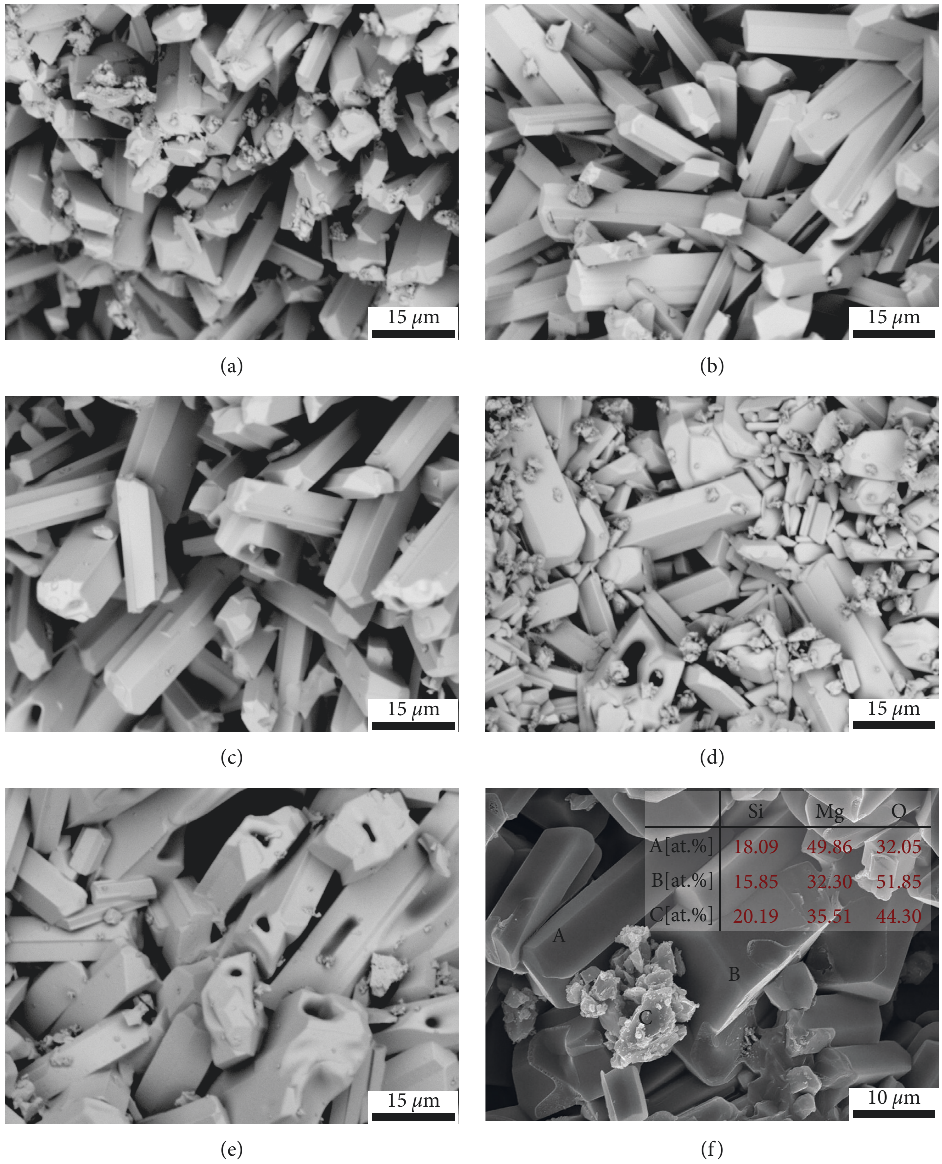

Figure 3: SEM images of $(Mg_{0.95}Cu_{0.05})_2SiO_4$ with 12% B_2O_3–LiF sintered at (a) 1000°C, (b) 1050°C, (c) 1100°C, (d) 1150°C, (e) 1200°C, and (f) EDS pattern of microdomain marked in Figure 3(d).

3. Results and Discussion

Figure 1(a) depicts the XRD patterns of $(Mg_{1-x}Cu_x)_2SiO_4$ ($x = 0.05$–0.20) ceramics sintered at 1350°C for 4 h. It could be seen that all the main diffraction peaks can be well indexed to the standard patterns of Mg_2SiO_4 (PDF#72–0296), indicating that the forsteritic-olivine solid solution with a single phase was formed. A very little protoenstatite Mg_2SiO_3 secondary phase appeared along with the main phase Mg_2SiO_4 in all compositions, which is similar to the results of Li et al. [10]. This result might be attributed to the fact that the amount of miscellaneous phase MgO is enough so that it could not react with $MgSiO_3$ to form Mg_2SiO_4. Moreover, as shown in Figure 1(b), with increasing the Cu content (x), the main peaks of Mg_2SiO_4 shift slightly toward lower angles, indicating an increase of unit-cell volume. Furthermore, the refined lattice parameters were also plotted as a function of Cu content (x) as shown in Figure 1(c), a near linear dependence between the lattice parameters (except c) and x value can be found, which is in agreement with the Vegard's law and also confirms the formation of a solid solution.

Figure 2 showed the bulk density of the $(Mg_{0.95}Cu_{0.5})_2SiO_4$ with 12% B_2O_3–LiF ceramics sintered at 1000°C was low, about 2.38 g/cm^2, but increased with increasing sintering temperature to a maximum value of 2.48 g/cm^2 for the specimen sintered at 1150°C and then reduced with a further increase in the temperature. The 12 wt.% H_3BO_3 added ceramics shows relative densities of 89%. The low density of magnesium silicate ceramics can be caused by two factors: the first is its crystallographic anisotropy, and the other is the hollow formed by the sintering agent at high temperature.

The SEM micrographs of the $(Mg_{0.95}Cu_{0.5})_2SiO_4$ with 12% B_2O_3–LiF ceramics sintered at 1000–1200°C for 4 h in air are shown in Figures 3(a)–3(e). Figure 3 shows that the

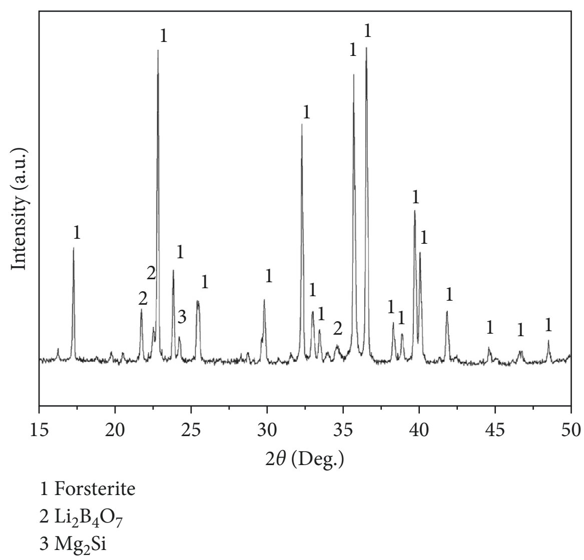

Figure 4: The XRD pattern of $(Mg_{0.95}Cu_{0.05})_2SiO_4$ with 12% B_2O_3–LiF sintered at 1150°C.

grains became lager and denser with increasing sintering temperature. Three types of grains were observed in the specimens of B_2O_3–LiF-doped $(Mg_{0.95}Cu_{0.5})_2SiO_4$ ceramics. In order to understand the distribution of the elements in the sample, the EDS of $(Mg_{0.95}Cu_{0.5})_2SiO_4$ with 12% B_2O_3–LiF ceramics sintered at 1150°C for 4 h is shown in Figure 3(f). The results presented the ratio of Mg : Si : O of rod-shaped grain (sport A and B) which is approximately 2 : 1 : 4, which agreed with the composition of forsterite. Li and coworkers also observed Mg_2SiO_4 with similar shape [10]. It seems impossible for the EDS detector to detect boron and lithium ions, which led to the restricted detection of B_2O_3–LiF. The small grains are to be Mg_2Si and $Li_2B_4O_7$, which is in accordance with the XRD analysis as shown in Figure 4.

Figure 5 showed the dielectric constant, quality factor, and τ_f of the $(Mg_{0.95}Cu_{0.5})_2SiO_4$ with 12% B_2O_3–LiF ceramics sintered at various temperatures for 4 h, respectively. The ε_r is mainly dominated by the structural characteristics, dielectric polarizability, and relative density of the ceramics [11–13]. It can be seen from Figure 5(a) that the variation trend of ε_r with sintering temperatures was not in agreement with that of relative density. It is noted that the sample had lower ε_r (4.37) when the sintering temperature was 1150°C. The $Q \times f$ values of the $(Mg_{0.95}Cu_{0.5})_2SiO_4$ with 12% B_2O_3–LiF ceramics sintered at 1000°C were low (15,000 GHz at 12.36 GHz) due to the low density, small grain size, and porous microstructure (as shown in Figure 3(a)). But, it increased with increasing sintering temperature to a value of 36,700 GHz for the specimen sintered at 1150 then seldom decreased to 32,600 GHz. The optimum sintering temperature was reduced by 200°C compared to the results of Li et al. Based on the classical dielectric theory, the value should increase as the grain size increases, because a reduction in the number of grain boundaries per unit volume would result in materials with a lower loss [12–15]. In fact, the ceramics had the highest $Q \times f$ values when the mean grain size of the ceramics was about 8~17 μm as shown in Figure 3.

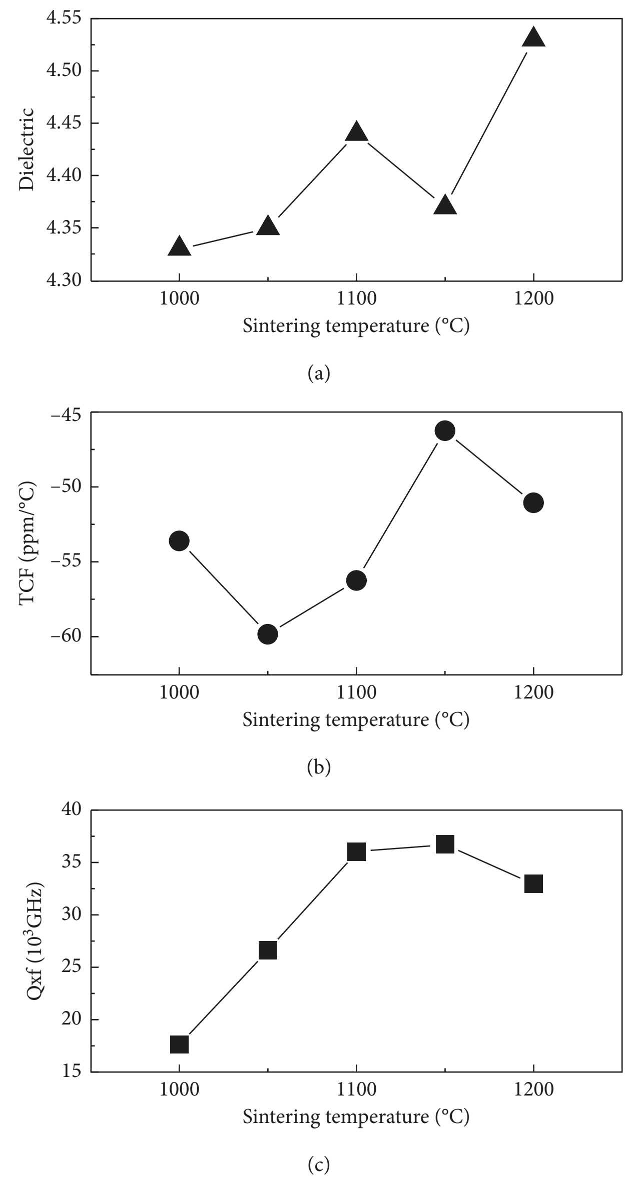

Figure 5: The dielectric constant ε_r, quality factor $Q \times f$, and temperature coefficient of resonant frequency τ_f of $(Mg_{0.95}Cu_{0.05})_2SiO_4$ with 12% B_2O_3–LiF as a function of sintering temperature.

Li et al. also observed similar result in our previous work [10]. This could be due to the interaction of various factors, such as distribution of element, porosity, grain size, presence of liquid-phase, and so on, which made it too difficult to reveal definitive remarks on grain size loss relationships [15–18]. The τ_f values of all ceramics, on the other hand, appeared to be a slight change (from −60~−40 ppm/°C) to sintering temperature, as shown in Figure 5. Generally, glass materials of lower melting temperature were mixed with the ceramic materials to degrade the sintering temperature. However, network formers contained in the glass ceramics may absorb the microwave power deeply at microwave frequency band, deteriorating the microwave performance for the material. Chang et al. reported that Li_3BO_3 ceramic possesses the microwave dielectric properties of $\varepsilon_r \sim 5$,

$Q \times f \sim 37{,}200$ GHz, and $\tau_f \sim 3.1$ ppm/°C [19]. In this work, the addition of 12 wt.% of B_2O_3–LiF effectively reduced the sintering temperature but worsened the microwave performance of the ceramic. It is an important task to explore the low sintering temperature, high density, and high-performance Mg_2SiO_4 ceramics in future work.

4. Conclusions

The microwave performance of $(Mg_{1-x}Cu_x)_2SiO_4$ ($x = 0.05$–0.20) ceramics were studied in terms of their microstructure and structural characteristics, as well as the sintering behavior. The results show that the Cu substitution not only obviously enhances the sintering activity but also improves the microwave performance of the ceramics. The $(Mg_{0.95}Cu_{0.5})_2SiO_4$ with 12% B_2O_3–LiF ceramics sintered at 1150°C for 4 h achieved excellent microwave dielectric properties of $\varepsilon_r = 4.37$, $Q \times f = 36{,}700$ GHz, and $\tau_f = -42.6$ ppm/°C. It can be used as a promising microwave substrate and LTCC material [20].

Conflicts of Interest

The authors declare that there are no conflicts of interests regarding the publication of this paper.

Acknowledgments

This work was supported by the National Natural Science Foundation of China (NSFC) (Project nos. 51272150, 51072110, and 51402235).

References

[1] C. Hu, Y. Liu, P. Liu, and B. Yang, "Novel low loss, low permittivity $(1-x)SiO_2 - xTiO_2$ + ywt% H_3BO_3, microwave dielectric ceramics for LTCC applications," *Journal of Alloys and Compounds*, vol. 712, pp. 804–810, 2017.

[2] H. Ohsato, T. Tsunooka, M. Ando, Y. Ohishi, Y. Miyauchi, and K. Kakimoto, "Millimeter-wave dielectric ceramics of alumina and forsterite with high quality factor and low dielectric constant," *Journal of the Korean Ceramic Society*, vol. 40, no. 4, pp. 350–353, 2003.

[3] T. Tsunooka, M. Androu, Y. Higashida, H. Sugiura, and H. Ohsato, "Effects of TiO_2, on sinterability and dielectric properties of high-Q, forsterite ceramics," *Journal of the European Ceramic Society*, vol. 23, no. 14, pp. 2573–2578, 2003.

[4] T. Tsunooka, H. Sugiyama, K. Kakimoto, H. Ohsato, and H. Ogawa, "Zero temperature coefficient τ_f and sinterability of forsterite ceramics by rutile addition," *Journal Ceramic Society of Japan*, vol. 112, pp. S1637–S1640, 2004.

[5] M. Ando, K. Himura, T. Tsunooka, I. Kagomiya, and H. Ohsato, "Synthesis of high-quality forsterite," *Japanese Journal of Applied Physics*, vol. 46, no. 10, pp. 7112–7116, 2007.

[6] M. Ando, H. Ohsato, I. Kagomiya, and T. Tsunooka, "Quality factor of forsterite for ultrahigh frequency dielectrics depending on synthesis process," *Japanese Journal of Applied Physics*, vol. 47, no. 9, pp. 7729–7731, 2008.

[7] H. Ohsato, "Millimeter-wave materials," in *Microwave Materials and Applications*, Chapter 5, M. T. Sebastian, R. Ubic, and H. Jantunen, Eds., Wiley, Hoboken, NJ, USA, 2017.

[8] T. S. Sasikala, C. Pavithran, and M. T. Sebastian, "Effect of lithium magnesium zinc borosilicate glass addition on densification temperature and dielectric properties of Mg_2SiO_4, ceramics," *Journal of Materials Science Materials in Electronics*, vol. 21, no. 2, pp. 141–144, 2010.

[9] C. Zhang, R. Zuo, J. Zhang, and Y. Wang, "Structure dependent microwave dielectric properties and middle temperature sintering of forsterite $(Mg_{1-x}Ni_x)_2SiO_4$ ceramics," *Journal of the American Ceramic Society*, vol. 98, no. 3, pp. 702–710, 2015.

[10] J. Li, P. Liu, Z. F. Fu, and Q. Q. Feng, "Microwave dielectric properties of low-fired $Mg_{1.9}Cu_{0.1}SiO_4$-$(La_{0.5}Na_{0.5})TiO_3$ composite ceramics," *Journal of Alloys and Compounds*, vol. 660, pp. 93–98, 2015.

[11] C. L. Pan, P. C. Chen, T. C. Tan, W. C. Lin, C. H. Shen, and S. H. Lin, "Low-temperature sintering and microwave dielectric properties of $CaWO_4$-Mg_2SiO_4 ceramics," *Advanced Materials Research*, vol. 933, pp. 12–16, 2014.

[12] K. X. Song and X. M. Chen, "Phase evolution and microwave dielectric characteristics of Ti-substituted Mg_2SiO_4, forsterite ceramics," *Materials Letters*, vol. 62, no. 3, pp. 520–522, 2008.

[13] N. W. J. Wan, H. Abdullah, and M. S. Zulfakar, "Effect of Zn site for Ca Substitution on optical and microwave dielectric properties of $ZnAl_2O_4$ thin films by sol gel method," *Advances in Materials Science and Engineering*, vol. 2014, Article ID 619024, 8 pages, 2014.

[14] Y. Wang, D. Zhou, Y. Zhang, and C. Chang, "Using multilayered substrate integrated waveguide to design microwave gain equalizer," *Advances in Materials Science and Engineering*, vol. 2014, Article ID 109247, 6 pages, 2015.

[15] C. Stergiou, "Microstructure and electromagnetic properties of Ni-Zn-Co ferrite up to 20 GHz," *Advances in Materials Science and Engineering*, vol. 2016, Article ID 1934783, 7 pages, 2016.

[16] L.-X. Pang and D. Zhou, "Microwave dielectric properties of low-firing Li_2MO_3 (M=Ti, Zr, Sn) ceramics with B_2O_3–CuO addition," *Journal of the American Ceramic Society*, vol. 93, no. 11, pp. 3614–3617, 2010.

[17] G. G. Yao, C. J. Pei, P. Liu, H. Y. Xing, L. X. Fu, and B. C. Liang, "Novel temperature stable $Ba_{1-x}Sr_xV_2O_6$, microwave dielectric ceramics with ultra-low sintering temperature," *Journal of Materials Science Materials in Electronics*, vol. 28, no. 18, pp. 13283–13288, 2017.

[18] J. Yang, X. Y. Deng, J. B. Li et al., "Broad and dielectric spectroscopy analysis of dielectric properties of barium titanate ceramics," *Advanced Materials Research*, vol. 744, pp. 323–328, 2013.

[19] S. Y. Chang, H. F. Pai, C. F. Tseng, and C. K. Tsai, "Microwave dielectric properties of ultra-low temperature fired Li_3BO_3, ceramics," *Journal of Alloys and Compounds*, vol. 698, pp. 814–818, 2017.

[20] M. T. Sebastian and H. Jantunen, "Low loss dielectric materials for LTCC applications: a review," *International Materials Reviews*, vol. 53, no. 2, pp. 57–90, 2008.